Tribology and Materials
Vol. 1, No. 2, 2022, pp. 70-80

ISSN 2812-9717
https://doi.org/10.46793/tribomat.2022.009

Optimisation of tensile stress of poly(lactic acid) 3D printed materials using response surface methodology

Miloš VORKAPIĆ [1,*], Ivana MLADENOVIĆ [1], Marija PERGAL [1], Toni IVANOV [2], Marija BALTIĆ [2]

[1] University of Belgrade, Institute of Chemistry, Technology and Metallurgy, Belgrade, Serbia
[2] University of Belgrade, Faculty of Mechanical Engineering, Belgrade, Serbia
*Corresponding author: worcky@nanosys.ihtm.bg.ac.rs

Keywords
additive manufacturing
fused deposition modelling
PLA
thermoplastic polymer
tensile testing
optimisation

History
Received: 22-05-2022
Revised: 05-06-2022
Accepted: 09-06-2022

Abstract
Three-dimensional printed plastic products developed through fused deposition modelling (FDM) take long-term mechanical loading in most industrial prototypes. This article focuses on the impact of the 3D printing parameters, type of thermal treatment and variation of characteristic dimensions of standard specimens on the tensile properties of poly(lactic acid) (PLA) material. Two mediums were used for thermal treatment: NaCl powder and plaster. The specimens immersed in NaCl powder were heated to the melting temperature of the filament (200 °C), while the processing of the plastered specimens was performed at a temperature of 100 °C. After treatment, the specimens were cooled at room temperature (25 °C), and the dimensions of the annealed and untreated specimens were controlled. The tensile test of the specimens was performed on the universal test machine. The response surface methodology (RSM) is employed to predict the tensile stress by undertaking input parameters. The analysis of variance (ANOVA) results revealed that the untreated specimens, orientation –45/45 and layer thickness of 0.1 mm had the highest tensile stress value. Thermal treatment in plaster showed a significant increase in tensile strength, while the best specimens were obtained after treatment in NaCl, and all refer to the –45/45 (0.1 mm) orientation.

1. Introduction

Additive manufacturing (AM) has helped many companies to save time during the designing process. AM enables rapid part realisation with complex geometry. Fused deposition modelling (FDM) is also a widely accepted AM technology. This technology is easy to use [1] and provides effortless model realisation, low maintenance costs, and affordable production of very complex models in a wide range of materials [2]. In this direction, the overall material cost is reduced, while the waste and use of ancillary tools are minimised [3].

FDM technology allows model modifications to be performed at any time until the beginning of the manufacturing process. These changes are easy to implement, as they only require CAD software, thus simplifying the communication with the customer. The CAD model is subsequently realised as a 3D object on a printer [4].

The FDM process involves melting the thermoplastic material through an extruder, see Fig. 1. The extruder transported filament to the guide via a stepper motor. Further, filament moves through the heater and leaves the nozzle as a molten material in a string form, after which it touches the active plate and sticks to it [5]. The extruder consists of two interconnected parts: (a) the hot part – which contains a nozzle and heater, and (b) the cold part or mechanism that cools and drives the hot part of the extruder.

The first layer is significant, and when it is formed in the XY plane, the extruder is moved by a specific value of the layer height on the *z*-axis, followed by the subsequent layer formation in the XY plane, and the procedure is repeated until the finished model of the desired height [7], see Fig. 1.

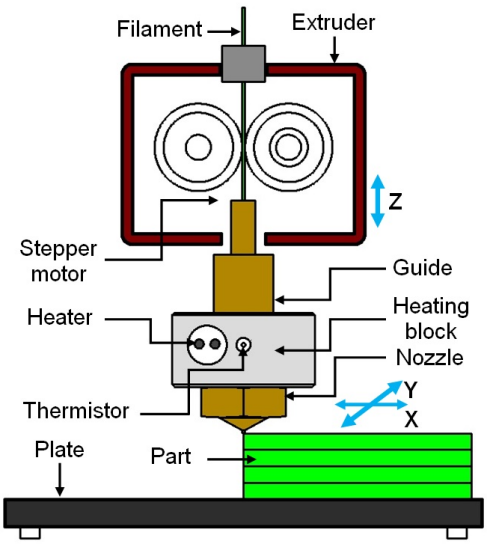

Figure 1. Layer formation process – Illustration; adapted from Vorkapić et al. [6], licensed under CC BY 4.0

The material is cooled and solidified as a printed element. The filament melting temperature (T_m) and the plate temperature (T_p) are critical. There is a risk that the cooling process across the layers will be nonlinear, which gives an irregular shape and incorrect geometry at the end. The temperature difference between the nozzle and the plate should be kept as small as possible.

The impact of layer thickness, orientation, air gap, raster width, and raster orientation on mechanical properties (flexural/tensile strength) was investigated by Panda et al. [8]. According to statistical analyses, they showed that all parameters (other than raster width) and the combinations of parameters were influential for tensile strength.

In the reference [9] authors investigated the impact of raster orientation of ABS part on the mechanical (tensile) properties. The result conducted those tensile properties (such as strength) was maximum and the same at (0/90) and (45/45) raster orientation.

Based on the experimental results, practical proposals were obtained for setting the expected parameters of the process concerning the mechanical properties [10]. The relationship between the main parameters of the process is given: stiffness and strength of PLA specimens obtained by the FDM process. As a deformation value, the thickness of the layer reaches its maximum at 0.15 mm and decreases as it approaches the value of 0.2 mm.

In the paper [11], the investigations were focused on boosting toughness and reducing the production cost of the FDM-printed tensile test specimens with the desired part thickness. Here, the tensile testing of specimens with a defined part thickness was performed. An artificial intelligence method – artificial neural network (ANN) and ANN – genetic algorithm (ANN-GA) were used to estimate toughness, part thickness and variables dependent on production costs.

According to the modelling results, it is necessary to improve the modelling accuracy by about 7.5, increase the thickness of the part by 11.5 and finally reduce the costs by 4.5 %. Also, the ANN algorithm, which uses Taguchi design, is a known tool for the tribological behaviour of aluminium composites [12-13], but in our case, it might be precious for further investigation of thermoplastic polymers.

The aim of this paper, in addition to PLA 3D printing of quality specimens and mechanical characterisation (tensile test) of the PLA material (treated/untreated), was also to investigate the impact factor of different 3D printing parameters (layer thickness, raster angle), annealing parameters (type of treatments or temperature of annealing), and specific dimension of specimens after treatment process on tensile stress values according to response surface methodology (RSM).

1.1 Printing material

Thermoplastic materials such as poly(lactic acid) PLA and poly(ethylene terephthalate) PET are most commonly used in the FDM process [14]. In this investigation, pure PLA filament was used. Pure PLA is widely available in the spool filament form of all colours, inexpensive, and the most widely used. Unfortunately, it has poor mechanical properties. PLA is a biodegradable, thermoplastic material. It has a relatively low melting temperature, 150 – 162 °C [15], which requires less printing energy. Unfortunately, this material is hygroscopic and not resistant to high temperatures [16]. The main physical and mechanical properties of PLA are given in Table 1 [17].

The PLA mechanical properties are significantly influenced by various technological variables, such as the nozzle diameter, layer thickness, infill percentage value, loaded specimen, and the filling rate and temperatures [18].

1.2 Response surface methodology

The FDM technology in various industrial applications is currently limited such to insufficient mechanical properties, poor surface quality, and

low dimensional accuracy. The setting of process parameters and their range depends on the section of FDM machines, filaments, nozzle dimensions, and the type of machine that determine the range of various parameters.

Table 1. PLA – physical and mechanical properties

Physical properties	
Density, g/cm^3	1.25
Extrusion temperature (T_e), °C	200
Glass transition temperature (T_g), °C	60
Mechanical properties	
Modulus of elasticity, GPa	3.5
Poisson ratio	0.36
Tensile strength, MPa	73
Shear modulus, GPa	1.28
Yield strength, MPa	49.6
Elongation, %	6

FDM is one of the most common techniques in additive manufacturing (AM) processes. It is necessary to obtain the optimum elements as discussed infill orientation, layer thickness, nozzle temperature, bed temperature, nozzle diameter and infill pattern. The proper parameter selection is crucial to produce good quality products with good mechanical properties, such as mechanical strength.

The paper [19] considered layer thickness, printing speed, print temperature and outer shell speed for PLA. Statistical analysis was performed using analysis of variance (ANOVA). Results are experimentally validated and compared with RSM. The flexural strength from experimental validation obtained using PSO exhibits an improvement of approximately 3.8 %.

In the paper [20], the influence of three FDM process parameters (air gap, raster angle, and build orientation) were considered on the flexural strength. The twelve nylon specimens were manufactured by the FDM process. Response surface methodology (RSM) was used as a statistical technique to analyse the results. The results indicate that the air gap and raster angle are the most influential parameters affecting flexural strength.

In the paper [21], layer height, print speed, print temperature, and outer shell speed were considered as input parameters. The surface roughness was the output response. The experimental design was carried out using the response surface methodology (RSM). The relationship between the input and output parameters was established using the regression model. The results showed that the surface roughness obtained using PSO and SOS had improved by about 8.5 and 8.8 %, respectively, compared with the conventional method, i.e. RSM. A good agreement was observed between the predicted surface roughness and the experimental values.

2. Experimental work

2.1 FDM manufacturing technology

The white PLA filament (manufacturer Wanhao) was used for the 3D printing specimens. The specimens were made according to the ASTM D638 [22] standard, which tests the tensile strength of plastics. According to mentioned standard, a series of specimens with a thickness of 3 mm and an initial distance between grips of 106 mm were considered, see Fig. 2.

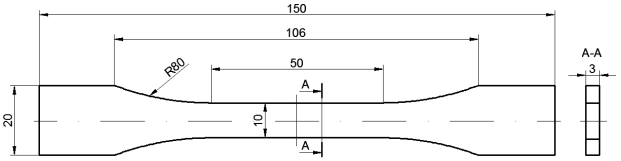

Figure 2. Dimensions of specimens (in mm) according to ASTM standard

Creating process begins with a 3D CAD model using CAD software packages. The model is implemented as a physical object using FDM technology, i.e. imported as *.stl file in the specialised “open source” program Ultimaker Cura 4.3.0, which sets the system's operating parameters.

The 3D printer Wanhao Duplicator i3 plus was used to manufacture specimens in this paper. The printer has a working volume of 200 × 200 × 180 mm print speed in the range of 10 to 100 mm/s. A PLA filament diameter of 1.75 mm was used, and the distance between the nozzle and the bed plate was set to 0.1 mm. The heater's maximum temperature usually reaches 280 °C (depending on the type of material). FDM technology realises a model by depositing molten material “layer by layer” through a nozzle. The printing parameters are displayed in Table 2.

Sixty specimens were made in this experiment, and twenty of them were used as reference or thermally untreated. Forty specimens were prepared for treatment (for moulding), namely: for immersion in NaCl powder (20 pieces) and submersion in plaster (20 pieces), see Table 3.

The specimens were made in a laboratory with a temperature of 25 °C and relative humidity of 55 % [23].

Table 2. Printing parameters

Parameter	Value
Layer height, mm	0.1 and 0.2
Wall line contour	3
Top layers	3
Bottom layers	3
Printing temperature, °C	210
Build plate temperature, °C	60
Printing speed, mm/s	50
Travel speed, mm/s	60
Infill density, %	100
Infill orientation, °	−45/45 and 90/0

Table 3. Specimens' classification

Treatment	Medium	Orientation, °	Layer thickness, mm	Specimen
Treated	Plaster	−45/45	0.1	1.1−5.1
			0.2	6.1−10.1
		90/0	0.1	11.1−15.1
			0.2	16.1−20.1
	NaCl powder	−45/45	0.1	21.1−25.1
			0.2	26.1−30.1
		90/0	0.1	31.1−35.1
			0.2	36.1−40.1
Untreated	Air	−45/45	0.1	41.1−45.1
			0.2	46.1−50.1
		90/0	0.1	51.1−55.1
			0.2	56.1−60.1

2.2 Moulding, annealing cooling and preparing for testing

The procedure took place in two directions: 1) immersing the specimens and moulding them with NaCl salt powder (see Fig. 3a) and 2) submerging and moulding the specimens in plaster (see Fig. 3b) [23].

The mould with specimens in NaCl powder was heated in an oven to 200 °C. Instrumentation dryer ST-01/02 (+ 50 °C to + 200 °C) was used. Ultrasonic bath Ultrasonic Cleaner – Acleaner (model 20, frequency 40 kHz) was used in plaster mould manufacturing to obtain complete adhesion of plaster over the entire specimen's surface and expel air from the emulsion.

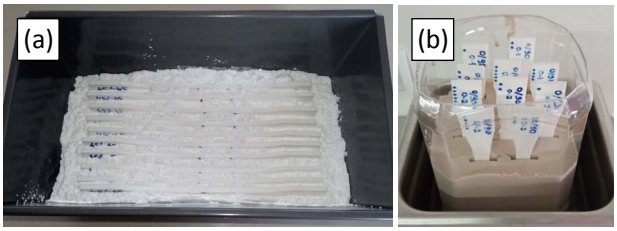

Figure 3. Specimen moulding: (a) in NaCl powder and (b) in plaster

The curing of the plaster mould took place at room temperature and lasted 24 h. It was performed to prevent mould cracking during drying in the oven. After curing the mould at room temperature, the Instrumentation ST-01/02 dryer was used to dry the mould further. The drying time of the specimen mould was six hours at 100 °C. Annealing heating treatment of the specimens immersed in plaster was performed at a temperature of 190 °C for 3 hours to achieve a temperature inside the mould of about 100 °C [23,24].

The specimens were removed from the moulds. After that, they were cleaned and prepared for testing the material's mechanical properties. The air gap between the layers is narrowed, and the surface's roughness is reduced [23]. That is, the layers and threads stuck together better in the material. Also, changes were observed on the surfaces of the specimens after annealing. Specimens taken from the mould with NaCl powder had traces of NaCl particles on their surface, while specimens taken from the plaster mould obtained a clear trace of the texture of the plaster.

2.3 Control of characteristic dimensions of the standard PLA specimens

During printing and temperature processes after printing in the different mediums, slight oscillations in the dimensions of the standard test specimens were noticed. The dimensions of the specimens are controlled and measured using a calliper. Characteristic dimensions of the specimens are marked in Figure 4, and values are given in Table 4.

The discussion section will explain why these changes occur. Three distinct measurement zones are marked in Figure 4 (middle, left and right zones), and the label *a* refers to the width, and *b* refers to the thickness of the test specimens (see section A-A).

The values in Table 4 are displayed as average values, measured on five specimens from the same series.

Table 4. Specimens dimension per series in the moulds*

T, °C	α	h, mm	a_l, mm	a_r, mm	a_m, mm	b_l, mm	b_r, mm	b_m, mm	L_u, mm
25	45	0.1	10.398	10.412	10.368	3.026	3.008	3.018	149.898
		0.2	10.424	10.392	10.410	3.066	3.054	3.056	150.026
	90	0.1	10.224	10.230	10.208	3.068	3.126	3.061	149.958
		0.2	10.424	10.420	10.412	3.172	3.148	3.076	149.974
100	45	0.1	10.258	10.312	10.290	3.106	3.098	3.101	149.144
		0.2	10.354	10.404	10.368	3.068	3.056	3.054	149.048
	90	0.1	10.268	10.278	10.262	3.104	3.090	3.078	149.354
		0.2	10.408	10.424	10.468	3.048	3.062	3.036	149.270
200	45	0.1	10.124	10.164	10.146	3.132	3.168	3.162	148.267
		0.2	10.306	10.304	10.308	3.124	3.114	3.128	148.568
	90	0.1	10.467	10.410	10.385	3.130	3.125	3.100	149.308
		0.2	10.352	10.346	10.356	3.102	3.004	3.178	149.246

*T – temperature of treatments; α – raster angle; h – layer thickness; a_l – width of specimen on the left side; a_r – width of specimen on the right side; a_m – width of specimen on the middle; b_l – depth of specimen on the left side; b_r – depth of specimen on the right side; b_m – depth of specimen on the middle; L_u – length of specimen.

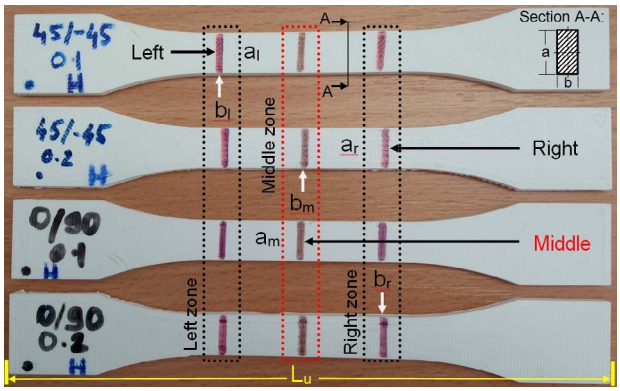

Figure 4. Test specimens impact dimension factors

2.4 Characterisation

The universal testing machine Shimadzu AGS-X with a maximum load capacity of 100 kN for tensile tests was used. Sixty specimens with 100 % filament infill were tested. Five specimens for every specimen series were printed in two print orientations (–45/45° and 0/90°) and two print layer thicknesses (0.1 and 0.2 mm).

The test procedure was performed in compliance with the ASTM D638 standard, where the specimens were tightened by non-shift wedge grips and force applied with a testing speed of 5 mm/min.

Trapezium Lite X software recorded real-time load force, displacement, and time data, after which the modulus of elasticity, maximum tensile stress and displacement were calculated from the obtained data. The stress and strain were calculated for every time step, after which the maximum values were obtained and averaged.

2.5 Optimisation

In this work, optimisation was used to observe the impact of each individual parameter on the stress value and was expressed through a mathematical model. Design-Expert v12 (Stat-Ease Inc.) software and optimal design was used for the response methodology to examine the correlation between the input variables and statistical analysis of the tensile testing results. The optimal design (OD) and central composite design (CCD) are a part of response surface methodology (RSM). It is a statistical technique useful for improving, developing, and optimising processes. The input parameters were classified into three categories: 1) printing parameters (raster angle and layer thickness), 2) medium parameters (type of the mediums or temperature in the mould) and 3) dimension parameters of standard specimens prior/after heat treatment (see Tables 4 and 5).

The output parameter or response was tensile stress, σ, obtained as maximum values on the universal test machine (see Table 6). The factors in this investigation were: temperature of treatments, printing parameters and dimensions of specimens. The levels were the values of these factors. Ten numerical factors with levels (codes as –1 for min. value and +1 for max. value), mean value and standard deviation are shown in Table 5.

Table 5. Factors and factor levels

Factors			Levels			
Name	Symbol	Unit	Coded low	Coded high	Mean	Standard deviation
Temperature	A: T	°C	−1 ↔ 25.00	+1 ↔ 200.0	108.33	74.870
Orientation	B: α	°	−1 ↔ 45.00	+1 ↔ 90.00	67.50	23.500
Layer thickness	C: h	mm	−1 ↔ 0.10	+1 ↔ 0.20	0.150	0.0522
Width left	D: a_l	mm	−1 ↔ 10.12	+1 ↔ 10.47	10.33	0.1006
Width right	E: a_r	mm	−1 ↔ 10.16	+1 ↔ 10.42	10.34	0.0849
Width middle	F: a_m	mm	−1 ↔ 10.15	+1 ↔ 10.47	10.33	0.0925
Depth left	G: b_l	mm	−1 ↔ 3.03	+1 ↔ 3.17	3.10	0.0414
Depth right	H: b_r	mm	−1 ↔ 3.00	+1 ↔ 3.17	3.09	0.0521
Depth middle	J: b_m	mm	−1 ↔ 3.02	+1 ↔ 3.18	3.09	0.0489
Specimen length	K: L_u	mm	−1 ↔ 148.27	+1↔ 150.03	149.34	0.5601

The model of the optimal design with three significant experimental factors and variations between them is given in Figure 5. The number of experimental runs was 12.

Figure 5 shows only some of the interactions between parameters and measurement values. Figure 5a shows the interaction between temperature in the different mediums and orientation (raster angle) on tensile stress value obtained on the standard test machine. Figure 5b interpreted the interaction between layer thickness and temperature, and Figure 5c is the model design for the interaction between orientation and layer thickness.

3. Results and discussion

3.1 Stress-strain analysis

The following Table 6 shows the average value for the maximum tensile stress for each specimen's combination. In the stress-strain analysis, annealing in plaster moulds increases the strength of the specimens on average by 12.7 %, while annealing in NaCl moulds increases the strength on average by 9.7 % compared to the reference specimens [23]. Interestingly, while annealing in plaster showed the most significant increase in maximum stress, annealing in NaCl moulds showed the most significant increase in modulus of elasticity due to good dispersion and uniform distribution of NaCl within the PLA matrix [23].

Heat treatment also appears to decrease the maximum elongation of test specimens before breaking with the average maximum displacement being around 6 – 7 % smaller than the untreated specimens [23]. Hence, though heat treatment in moulds led to increases of strength and material became more brittle.

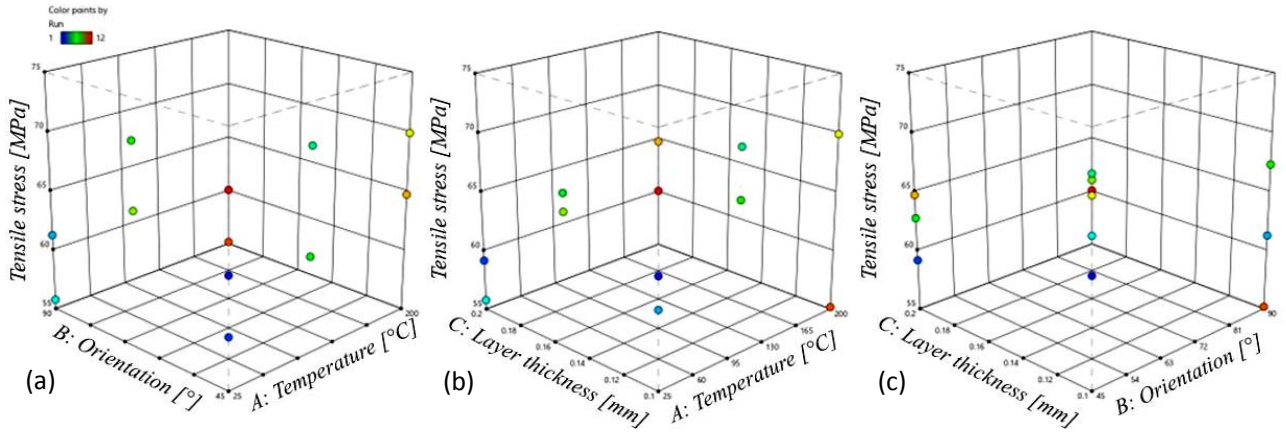

Figure 5. Model of optimal design for stress with the interaction between factors: (a) temperature and orientation, (b) temperature and layer thickness and (c) orientation and layer thickness

Table 6. Specimen combinations for the average value of maximum tensile stress

No.	Raster angle; Layer height	Treatment	Specimens	Maximum tensile stress, MPa
1	45/–45; 0.1 mm	Plaster	1.1–5.1	71.66
		NaCl powder	21.1–25.1	70.08
		Air	41.1–45.1	64.08
2	45/–45; 0.2 mm	Plaster	6.1–10.1	62.97
		NaCl powder	26.1–30.1	64.95
		Air	46.1–50.1	59.31
3	0/90; 0.1 mm	Plaster	11.1–15.1	67.53
		NaCl powder	31.1–35.1	61.48
		Air	51.1–55.1	55.79
4	0/90; 0.2 mm	Plaster	16.1–20.1	61.25
		NaCl powder	36.1–40.1	60.24
		Air	56.1–60.1	54.81

3.2 Statistical analysis of tensile stress

Results of ANOVA for tensile stress response are shown in Table 6. The mathematical model (linear) of the response surface methodology for tensile stress (σ) was presented in Equation (1). All factors in coded forms are specified in Table 7. The coded equation is useful for selecting the parameters' relative impact according to the factor coefficients' values.

$$\begin{aligned}\text{Stress}(\sigma) = {} & 64.84 + 11.34\,A - 3.62\,B - \\ & -2.01\,C - 27.77\,D - 5.52\,E + 20.87\,F + \\ & +11.89\,G - 7.32\,H - 14.37\,J + 10.72\,K,\end{aligned} \quad (1)$$

where A, B, C, D, E, F, G, H, J and K represent numerical factors from Table 5 corresponding to the input variables, i.e. temperature, orientation, layer thickness, width (left, right and middle), depth (left, right and middle) and length of specimens.

The statistical *p*-value is an important value that describes the significance of the defined factors' impact on the measured response, which is in our case the stress of the 3D printing PLA materials, treated or untreated in the mould of salt or plaster. The factor is considered as impacting for a *p*-value below 0.05, and above 0.05 its influence is negligible [25]. Besides, input parameters have different contributions that define their weight in the statistical model. A, B, C, D, E, F, G, H, J, K are significant model terms. Values greater than 0.1000 indicate the model terms are not significant. If there are many insignificant model terms (not counting those required to support hierarchy), model reduction may improve the model. Fisher's statistical tests (*F*-value) found for stress high value, which shows that the prediction is useful. The model *F*-value of 141330.78 implies the model is significant. There is only a 0.21 % chance that a large *F*-value could occur due to noise.

From Table 7, it can be concluded that all parameters significantly impacted the stress value. The influence of all parameters on the tensile stress of annealing or untreated 3D printing PLA specimens can be presented in the form of 2D diagrams (Fig. 6). From Equation (1) and Figure 6 (tilt of the line), a trend of stress variation with one-factor change can be seen.

Table 7. Analysis of variance for tensile stress value (*p* – probability; DOF – degree of freedom)

Source	Sum of square	DOF	Mean square	*F*-value	*p*-value	Remark
Model	290.41	10	29.04	1.413E+05	0.0021	significant
A: Temperature	3.47	1	3.47	16894.49	0.0049	
B: Orientation	12.14	1	12.14	59103.44	0.0026	
C: Layer thickness	8.32	1	8.32	40510.80	0.0032	
D: Width left	9.47	1	9.47	46081.89	0.0030	
E: Width right	2.12	1	2.12	10312.69	0.0063	
F: Width middle	21.16	1	21.16	1.030E+05	0.0020	
G: Depth left	18.28	1	18.28	88970.84	0.0021	
H: Depth right	24.07	1	24.07	1.171E+05	0.0019	
J: Depth middle	9.07	1	9.07	44134.95	0.0030	
K: Specimen length	2.12	1	2.12	10336.87	0.0063	
Residual	0.0002	1	0.0002			
Corrected total	290.41	11				

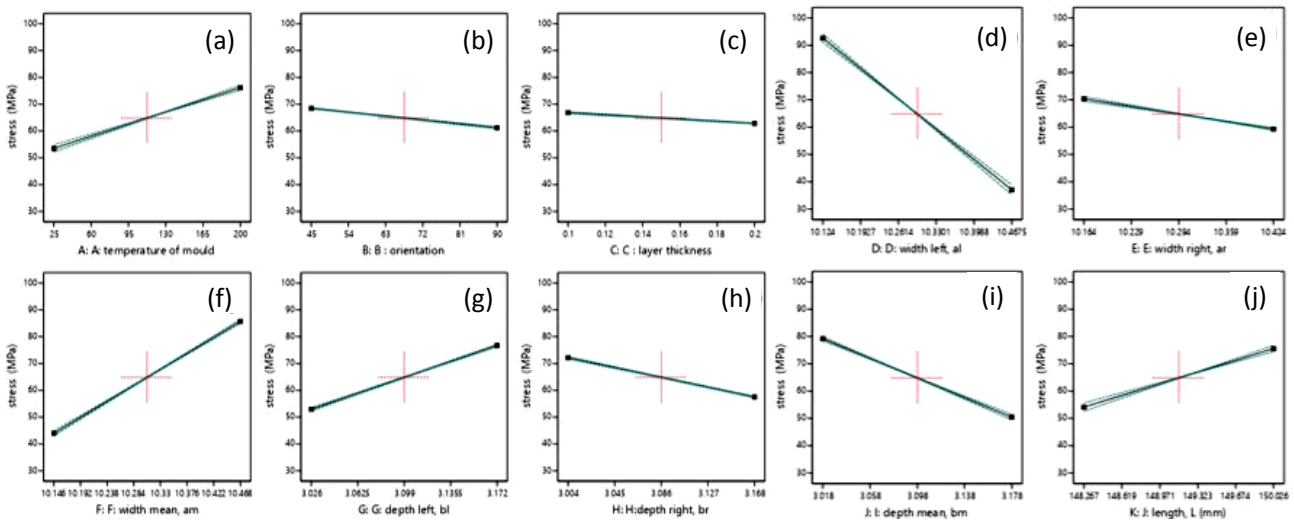

Figure 6. The influence of each input parameters on tensile trends: (a) temperature, (b) orientation, (c) layer thickness, (d) width left, (e) width right, (f) width middle, (g) depth left, (h) depth right, (i) depth middle and (j) specimen length

With the increase of temperature from 25 °C (untreated specimens) to 200 °C (treated specimens in the salt mould), the tensile stress also increased. The room temperature condition (25 °C) results in reduced bonding between two printing layers, leading to a lower tensile stress value. An increase of temperature value might trend to enhance polymer chain mobility that controls the crystallisation capacity of the polymer [25]. The PLA polymer in rigid and brittle form can be demonstrated as a material with low stress value. The increase in tensile stress properties can be explained through the material's viscosity reduction [26]. The specimens treated in the mould have higher masses than untreated specimens. The immersing of the PLA material in different mediums resulted in a reduction of surface roughness and a reduction of air gaps between layers [23].

Figure 7 shows the influence of two parameters on stress value together in the form of 3D graphs, while the average value of other parameters was chosen as constant. Although the temperature is not one crucial and dominant factor in the impact on the tensile stress, it was chosen to observe the temperature of the process in combination with the factors of the 3D printing (orientation and layer thickness, see Figs. 7a and 7c) and specimen dimensions (depth middle and length, see Figs. 7c and 7d).

From Figures 7a, 7b and 7c, it can be concluded that the temperature in the mould had the most significant impact on tensile stress. On the other hand, rising temperatures cause as a consequence changes in the dimensions of the specimens. The interaction of the layer thickness and printing orientation had a slight impact on the tensile stress. The flat plotted surface area was shown in Figures 7a and 7b. These results are in line with the published literature [23]. Lower layer thickness provides good mechanical strength and low stress. As the layer thickness decreases, the bonding between the layers strengthens, resulting in an improved mechanical feature [27]. In Figure 8c, the tensile stress for linear pattern increases slightly with an increase in temperature, while it decreases with an increase in the depth of specimen measurement in the middle zone on the neck, from a low level to a high level. The shorter and thicker

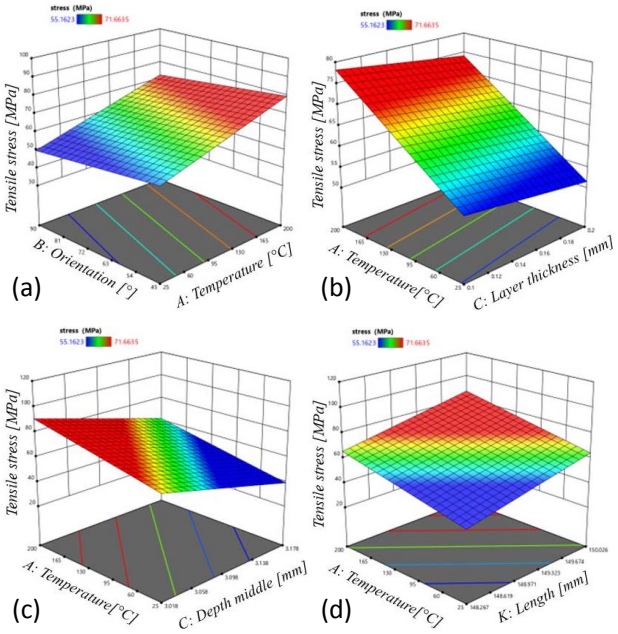

Figure 7. The simultaneous influence of temperature in the mould and: (a) printing orientation, (b) printing layer thickness, (c) depth in the middle of specimens and (c) length of specimens on tensile stress values

specimens tend to be more ductile, regardless of the application of the treatment. Thermal treatment in plaster and salt modes only integrates this trend regarding the impact of dimension.

Figure 8 shows the predicted response of stress values vs. the actual (experimental) stress value points distributed along a 45° line. The organised model is adequate and satisfactory. It was found that the tensile stress is predicted by applying the simple linear regression model with a maximum deficient error. The probability values less than 0.050 and the determination coefficient (R^2) evaluating the correlation between experimental and predicted values of 0.9989 indicate that this model is successfully applied. The attained excellent agreement between these values of stress shows that the RSM is a suitable tool for optimising the 3D printing processes to obtain PLA specimen of desired characteristics, in this case, tensile stress.

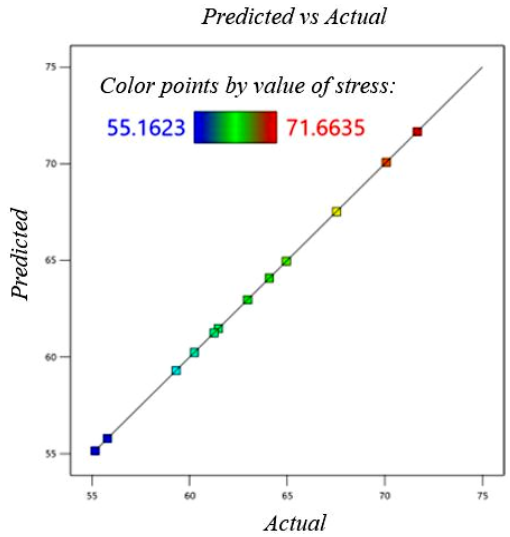

Figure 8. Predicted response vs. the actual values for tensile stress for 3D PLA specimens obtained after annealing in the moulds

4. Conclusion

The effects of ten different parameters (two printing, one annealing and seven dimensions parameters) on the tensile stress values of the referent and treated PLA specimens in the salt and plaster mould were presented. For the investigation of the impacts of all parameters, an optimal, random design was used. Increasing the parameters such as temperature in the mould, the width of the specimen in the middle zone, depth of the specimen in the left zone and length resulted in increased tensile stress.

Decreasing the values of the following parameters: layer thickness, raster angle, width in the correct zone, and depth in the right and middle zone of the PLA specimen increased stress, too. The type of annealing mould or temperature inside strongly affected the stress value. The annealing treatment in the plaster or salt moulds of PLA specimen improved tensile properties such as tensile strength with a better connection between layers and reduced voids between them. Therefore, increasing the layer thickness (decreasing the number of layers) resulted in better tensile properties.

The lower tensile strength was obtained in untreated specimens but with increasing tensile stress and elongation. It was shown that heat treatment of the specimens increases strength, with treatment in plaster providing the best results (12.7 % increase in maximum tensile stress). The best increase in tensile strength was obtained in the plaster-treated specimens with an orientation 0/90 and layer thickness 0.1mm (21 % increase in maximum tensile stress). Also, it was shown that there is a decrease in plasticity obtained with both annealing methods making the specimens more brittle. In addition, an increase in elasticity was obtained with both mould treatments. Using response surface methodology, a simple linear multi-parameter model for predicted tensile stress was generated. The determination coefficient of 0.9989 was calculated. Excellent agreement between experimental and predicted values of tensile stress was established.

Acknowledgement

This work was financially supported by the Ministry of Education, Science and Technological Development of the Republic of Serbia, Grants No. 451-03-68/2022-14/200026 and 451-03-68/2022-14/200105.

References

[1] T.D. Ngo, A. Kashani, G. Imbalzano, K.T.Q. Nguyen, D. Hui, Additive manufacturing (3D printing): A review of materials, methods, applications and challenges, Composites Part B: Engineering, Vol. 143, 2018, pp. 172-196, DOI: 10.1016/j.compositesb.2018.02.012

[2] J.R.C. Dizon, A.H. Espera Jr., Q. Chen, R.C. Advincula, Mechanical characterization of 3D-printed polymers, Additive Manufacturing, Vol. 20, 2018, pp. 44-67, DOI: 10.1016/j.addma.2017.12.002

[3] M. Gebler, A.J.M. Schoot Uiterkamp, C. Visser, A global sustainability perspective on 3D printing

technologies, Energy Policy, Vol. 74, 2014, pp. 158-167, DOI: 10.1016/j.enpol.2014.08.033

[4] T. Campbell, C. Williams, O. Ivanova, B. Garrett, Could 3D printing change the world?, available at: https://www.atlanticcouncil.org/in-depth-research-reports/report/could-3d-printing-change-the-world, accessed: 05.06.2022.

[5] K. Bassett, R. Carriveau, D.S.-K. Ting, 3D printed wind turbines part 1: Design considerations and rapid manufacture potential, Sustainable Energy Technologies and Assessments, Vol. 11, 2015, pp. 186-193, DOI: 10.1016/j.seta.2015.01.002

[6] M.D. Vorkapić, T.D. Ivanov, M.Z. Baltić, D.D. Kreculj, D.Lj. Tanović, A.M. Kovačević, Upotreba 3D štampe u analizi dizajna realizovanog proizvoda: Slučaj – kutija malogabaritnog transmitera pritiska [The usage of 3D printing in the analysis of the product design: Case – electronic enclosure of compact pressure transmitter], Tehnika, Vol. 75, No. 2, 2020, pp. 179-186, DOI: 10.5937/Tehnika2002179v [in Serbian].

[7] J. Jiang, Y.-F. Fu, A short survey of sustainable material extrusion additive manufacturing, Australian Journal of Mechanical Engineering, Article in Press, DOI: 10.1080/14484846.2020.1825045

[8] S.K. Panda, S. Padhee, A.K. Sood, S.S. Mahapatra, Optimization of fused deposition modelling (FDM) process parameters using bacterial foraging technique, Intelligent Information Management, Vol. 1, No. 2, 2009, pp. 89-97, DOI: 10.4236/iim.2009.12014

[9] A.W. Fatimatuzahraa, B. Farahaina, W.A.Y Yusoff, The effect of employing different raster orientations on the mechanical properties and microstructure of fused deposition modeling parts, in Proceedings of the 2011 IEEE Symposium on Business, Engineering and Industrial Applications (ISBEIA), 25-28.09.2011, Langkawi, Malaysia, 22-27, DOI: 10.1109/ISBEIA.2011.6088811

[10] A. Lanzotti, M. Grasso, G. Staiano, M. Martorelli, The impact of process parameters on mechanical properties of parts fabricated in PLA with an open-source 3-D printer, Rapid Prototyping Journal, Vol. 21, No. 5, 2015, pp. 604-617, DOI: 10.1108/RPJ-09-2014-0135

[11] M.S. Meiabadi, M. Moradi, M. Karamimoghadam, S. Ardabili, M. Bodaghi, M. Shokri, A.H. Mosavi, Modeling the producibility of 3D printing in polylactic acid using artificial neural networks and fused filament fabrication, Polymers, Vol. 13, No. 19, 2021, Paper 3219, DOI: 10.3390/polym13193219

[12] B. Stojanović, A. Vencl, I. Bobić, S. Miladinović, J. Skerlić, Experimental optimisation of the tribological behaviour of Al/SiC/Gr hybrid composites based on Taguchi's method and artificial neural network, Journal of the Brazilian Society of Mechanical Sciences and Engineering, Vol. 40, No. 6, 2018, Paper 311, DOI: 10.1007/s40430-018-1237-y

[13] B. Stojanović, R. Tomović, S. Gajević, J. Petrović, S. Miladinović, Tribological behavior of aluminum composites using Taguchi design and ANN, Advanced Engineering Letters, Vol. 1, No. 1, 2022, pp. 28-34, DOI: 10.46793/adeletters.2022.1.1.5

[14] N. Guo, M.C. Leu, Additive manufacturing: Technology, applications and research needs, Frontiers of Mechanical Engineering, Vol. 8, No. 3, 2013, pp. 215-243, DOI: 10.1007/s11465-013-0248-8

[15] S. Farah, D.G. Anderson, R. Langer, Physical and mechanical properties of PLA, and their functions in widespread applications – A comprehensive review, Advanced Drug Delivery Reviews, Vol. 107, 2016, pp. 367-392, DOI: 10.1016/j.addr.2016.06.012

[16] M.S. Hasan, T. Ivanov, M. Vorkapic, A. Simonovic, D. Daou, A. Kovacevic, A. Milovanovic, Impact of aging effect and heat treatment on the tensile properties of PLA (poly lactic acid) printed parts, Materiale Plastice, Vol. 57, No. 3, 2020, pp. 147-159, DOI: 10.37358/MP.20.3.5389

[17] P.M. Cardoso Carneiro, P. Gamboa, Structural analysis of wing ribs obtained by additive manufacturing, Rapid Prototyping Journal, Vol. 25, No. 4, 2019, pp. 708-720, DOI: 10.1108/RPJ-02-2018-0044

[18] M. Fernandez-Vicente, W. Calle, S. Ferrandiz, A. Conejero, Effect of infill parameters on tensile mechanical behavior in desktop 3D printing, 3D Printing and Additive Manufacturing, Vol. 3, No. 3, 2016, pp. 183-192, DOI: 10.1089/3dp.2015.0036

[19] M.S. Saad, A.M. Nor, M.Z. Zakaria, M.E. Baharudin, W.S. Yusoff, Modelling and evolutionary computation optimization on FDM process for flexural strength using integrated approach RSM and PSO, Progress in Additive Manufacturing, Vol. 6, No. 1, 2021, pp. 143-154, DOI: 10.1007/s40964-020-00157-z

[20] S.N. Kamoona, S.H. Masood, O.A. Mohamed, Experimental investigation on flexural properties of FDM processed Nylon 12 parts using RSM, IOP Conference Series: Materials Science and Engineering, Vol. 377, 2018, Paper 012137, DOI: 10.1088/1757-899X/377/1/012137

[21] M.S. Saad, A.M. Nor, M.E. Baharudin, M.Z. Zakaria, A.F. Aiman, Optimization of surface

roughness in FDM 3D printer using response surface methodology, particle swarm optimization, and symbiotic organism search algorithms, The International Journal of Advanced Manufacturing Technology, Vol. 105, No. 12, 2019, pp. 5121-5137, DOI: 10.1007/s00170-019-04568-3

[22] ASTM D638-14, Standard Test Method for Tensile Properties of Plastics, 2014.

[23] M. Vorkapić, I. Mladenović, T. Ivanov, A. Kovačević, M.S. Hasan, A. Simonović, I. Trajković, Enhancing mechanical properties of 3D printed thermoplastic polymers by annealing in moulds, Advances in Mechanical Engineering, Vol. 14, No. 8, 2022, DOI: 10.1177/16878132221120737

[24] C.G. Amza, A. Zapciu, G. Constantin, F. Baciu, M.I. Vasile, Enhancing mechanical properties of polymer 3D printed parts, Polymers, Vol. 13, No. 4, 2021, Paper 562, DOI: 10.3390/polym13040562

[25] P.A. Eutionnat-Diffo, Y. Chen, J. Guan, A. Cayla, C. Campagne, X. Zeng, V. Nierstrasz, Stress, strain and deformation of poly-lactic acid filament deposited onto polyethylene terephthalate woven fabric through 3D printing process, Scientific Reports, Vol. 9, 2019, Paper 14333, DOI: 10.1038/s41598-019-50832-7

[26] D. Godec, S. Cano, C. Holzer, J. Gonzalez-Gutierrez, Optimization of the 3D printing parameters for tensile properties of specimens produced by fused filament fabrication of 17-4PH stainless steel, Materials, Vol. 13, No. 3, 2020, Paper 774, DOI: 10.3390/ma13030774

[27] V. Kovan, G. Altan, E.S. Topal, Effect of layer thickness and print orientation on strength of 3D printed and adhesively bonded single lap joints, Journal of Mechanical Science and Technology, Vol. 31, No. 5, 2017, pp. 2197-2201, DOI: 10.1007/s12206-017-0415-7